

# ADJUHand - A Passive Anthropomorphic Hand Model with Adjustable Finger Stiffness for Exoskeleton Evaluation

Nico G. M. Weber, Sebastian Dietz, Jonas Walter, Dominik I. Braun, Alessandro Del Vecchio, Jörg Franke

**Abstract**—Each year, more than 12 million strokes and nearly one million spinal cord injuries occur worldwide. These conditions can cause severe hand impairments, leading to a significant loss of independence. Hand exoskeletons have emerged as a promising solution to support the restoration of grasping function in both rehabilitation settings and daily life. However, testing such devices remains a major challenge during the development phase. Existing hand models are either overly simplistic, lacking anatomical realism or articulation, or are complex active prosthetic systems that are costly, difficult to replicate, and not designed for passive actuation. Testing on healthy individuals introduces safety risks and bias, as their hands behave differently and may unconsciously assist movement. Moreover, direct patient testing is resource-intensive and limited. This paper presents the ADJUHand, a passive anthropomorphic hand model designed to facilitate testing of hand exoskeletons. The ADJUHand can be fabricated easily using a standard FDM 3D printer, a few screws and springs. Motion capture experiments demonstrate that the fingers follow anatomically accurate flexion trajectories with a total finger flexion angle of 249.9°. Furthermore, the stiffness of each finger can be adjusted to simulate varying levels of joint rigidity, as observed in individuals with spastic or stiff fingers. Additionally the ADJUHand enables finger abduction and thumb circumduction, facilitating diverse grasp configurations.

## I. INTRODUCTION

Neurological and musculoskeletal disorders such as stroke, which affects around 12 million people globally each year [1], or spinal cord injuries, with nearly one million cases annually worldwide [2], can severely impair the functionality of the human hand [3], [4]. Given the hand's vital role in nearly all aspects of daily life, such impairments often cause a significant loss of independence and a considerable psychological burden, further impacting quality of life [3].

One promising approach to restore or support hand functions in rehabilitation and daily life involves the use of hand exoskeletons. Hand exoskeletons, also called wearable robots or active orthoses, involve mechatronic often glove-like structures attached to the users hand to support or restore the hand and finger movements. Numerous studies have demonstrated this on impaired users in controlled laboratory settings and clinical environments [5], [6].

Although many research groups are exploring a variety of technologies for hand exoskeletons [7], [8], there is still a

N. G. M. Weber, S. Dietz, J. Walter and J. Franke are with Institute for Factory Automation and Production Systems, Friedrich-Alexander-Universitaet Erlangen-Nuernberg, Germany (email: nico.weber@faps.fau.de).

D. I. Braun and A. Del Vecchio are with Department Artificial Intelligence in Biomedical Engineering, Friedrich-Alexander-Universitaet Erlangen-Nuernberg, Germany (email: alessandro.del.vecchio@fau.de).

This work was supported by Bavarian Ministry of economic Affairs, Regional development and energy (StMWi) grant Mv- 2303-0006.

lack of accessible, reliable and standardized tools for testing and evaluating these devices [9], [10], [11].

Hand exoskeletons are tested using three different approaches: on healthy hands, on paralyzed hands or on anatomical models, with the majority of studies conducting tests on healthy participants [11]. However, this approach carries inherent safety risks for the participants and presents significant challenges in obtaining reliable evaluation results [10]. It is often difficult to rule out whether the finger movements are solely induced by the exoskeleton or whether the subject is subconsciously assisting [9]. During testing our own exoskeleton, we noticed that even unbiased participants tend to contribute involuntarily. Only with substantial additional effort, such as using electromyography to measure muscle activity, can such assistance be detected and quantified [12].

A second issue arises from the anatomical differences between a paralyzed and a healthy hand. Even if an exoskeleton performs well on a healthy subject, its performance cannot be directly translated to impaired hands, which behave differently. Conditions such as muscle atrophy, joint contractures and spasticity result in fundamentally altered biomechanics [13], [14].

The most accurate and clinically relevant evaluation can only be achieved through direct testing with individuals with hand impairments. However, beyond the previously mentioned safety concerns, such testing is also hindered by limited participant availability and is typically time consuming, costly, and infrequent [10].

The third and safest approach involves testing on passive hand models. However, commercially available models often don't include movable joints or are overly simplified, lacking anatomical accuracy. Other models [15] feature high anatomical detail, which complicates reproduction and results in a fragile design due to the absence of a skin-like outer layer, making them unsuitable as a testing device.

Active hand models, such as prosthetic hands, could theoretically be used, but they are designed for an entirely different purpose and are not suitable for passive movement. Internal motor resistance and control mechanisms make them inappropriate for this application [9]. Furthermore, such prosthetic systems are often expensive, adding an additional barrier to their use in early-stage testing.

There are only a few publications that propose a passive anthropomorphic hand model specifically designed for the evaluation of hand exoskeletons [9], [10], [16]. However, those approaches fail to replicate key characteristics of paralyzed hands, lacking increased finger stiffness, offering only

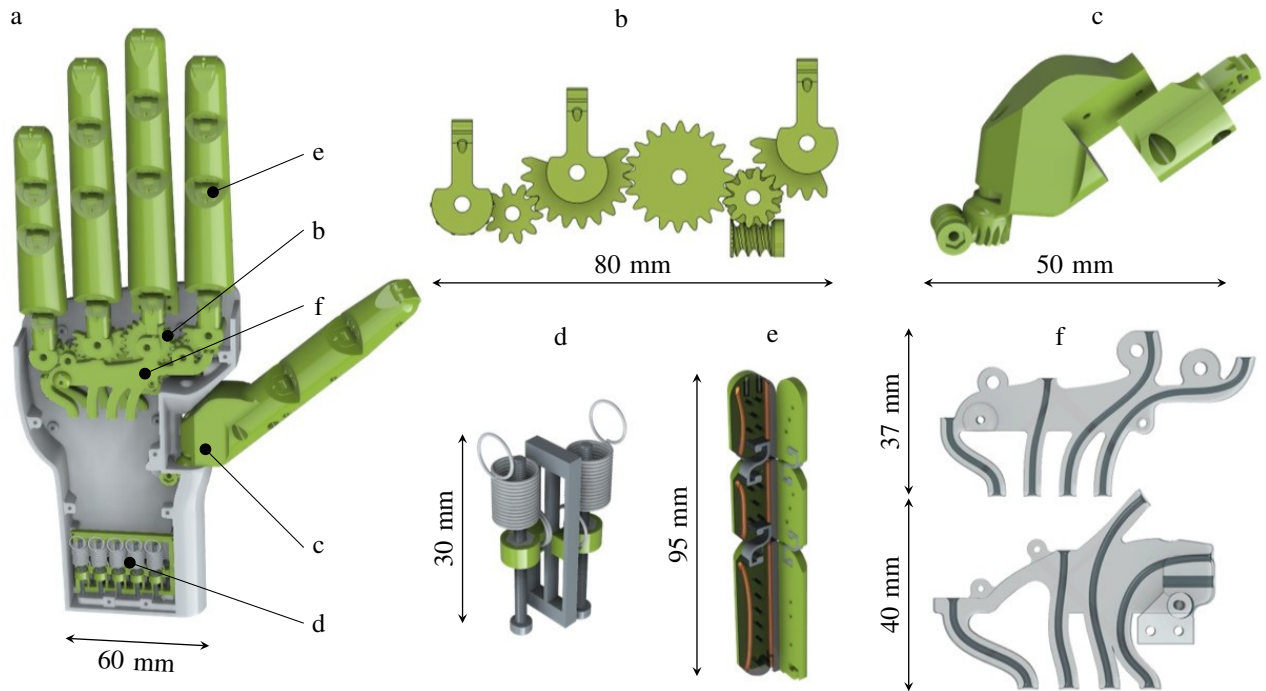


Fig. 1. Design overview of the ADJUHand (a) ADJUHand with palmar plate removed. (b) Gear system for finger abduction and adduction. (c) Gear mechanism for thumb circumduction. (d) Spring mechanism for tensioning palmar and dorsal tendons to adjust finger stiffness. (e) Cutaway view of a finger with rolling contact joints (white) and internal cable routing (orange). (f) Internal cable routing parts for palmar (top) and dorsal (bottom) tendons.

cumbersome adjustments for finger abduction and adduction, and being difficult to reproduce, which limits their suitability for practical and realistic testing scenarios.

Here we present a passive anthropomorphic hand model, the ADJUHand, with adjustable finger stiffness and configurable finger abduction and adduction to address the question of whether such a model can serve as a realistic, adaptable and safe platform for evaluating hand exoskeletons.

## II. MATERIALS AND METHODS

The following section presents a detailed overview of the ADJUHand's design, focusing on its dimensional characteristics, joint architecture, the abduction and adduction mechanism, and the adjustable stiffness system. Subsequently, the methods used to assess the kinematics and mechanical properties are presented, including motion capturing for movement analysis and force measurements for evaluating finger stiffness.

### A. Hand Design

The outer layout and dimensions of the ADJUHand was defined based on anthropometric data from [17], [18], and [19], supplemented by reasonable assumptions such as uniform spacing between the fingers, which allowed for the accurate placement of the metacarpophalangeal (MCP) joints of each digit within the system. To achieve both adjustability and anatomically inspired motion, the ADJUHand incorporates four distinct mechanical subsystems: rolling contact joints (see Fig. 1e), a gear system for finger abduction and adduction (see Fig. 1b), a separate gear mechanism enabling thumb

circumduction (see Fig. 1c), and an adjustable stiffness system comprising tendon routing (see Fig. 1f) and a spring mechanism to pretension the internal palmar and dorsal tendons (see Fig. 1d).

### B. Finger Joint Design

For the finger joints of the ADJUHand, 3D-printed rolling contact joints are used due to their inherently low resistance to movement, similar to the human synovial joints [20], as well as their compact and easy to manufacture design and long-term wear resistance [21]. Each rolling contact joint consist of three 3D-printed thermoplastic polyurethane (TPU) inserts, which are embedded into the 3D-printed polylactic acid (PLA) structure of the finger phalanges, connecting them to each other and linking the fingers to the main body of the ADJUHand (see Fig. 1e). During preliminary testing, the rolling contact joints underwent up to 10,000 actuation cycles without any signs of material fatigue or structural changes in the joint.

### C. Finger Abduction and Thumb Circumduction Design

To achieve finger abduction, a gear train was designed to enable radialduction of the index finger in tandem with ulnaruction of the ring and little fingers (see Fig. 1b). The gear ratios are chosen such that the little finger moves twice the angular distance of the ring finger, while the index finger moves the same distance as the ring finger in the opposite direction, thereby abducting the fingers. The middle finger is fixed to the casing of the ADJUHand and remains in place.

The driving force is introduced via a worm drive connected to the system of spur gears.

A similar worm drive mechanism is used to generate the rotational motion required for thumb circumduction. Approximating the thumb's movement as purely rotational allows direct integration of the worm gear into the thumb's base component, which can swivel up to a circumduction angle of  $95^\circ$  (see Fig. 1c). This design ensures that the fingers remain in position after actuation, even under external forces, due to the self-locking property of the worm drive.

Each worm drive is actuated by a screw onto which a 3D-printed worm component is mounted. The screw-nut arrangement ensures secure mechanical coupling and prevents unwanted translational movement.

#### D. Finger Stiffness System

The stiffness for flexion and extension of each finger can be adjusted independently via a tensioner unit at the proximal end of the ADJUHand (see Fig. 1d). This unit consists of ten springs, each arranged coaxially around a screw and connected to the screw threads through coupling elements that interlock with guiding rails to prevent rotation. Turning the screws linearly adjusts the tension in the springs, which is transmitted to palmar (for extension stiffness) or dorsal (for flexion stiffness) tendons running through the hand and fingers. To prevent interference between the abduction mechanism's gears and the tendons, their paths are routed through dedicated cable guides (see Fig. 1f).

#### E. Finger Kinematics Evaluation with Motion Capturing

Motion capturing was performed in order to gain insight into the range of motion of the different subsystems of the hand model. Using a setup consisting of ten *OptiTrack Prime<sup>x</sup>22* motion capturing cameras the flexion of the index finger, the abduction of the long fingers and the circumduction of the thumb were tracked and evaluated. To analyze finger flexion, seven optical markers were placed on the ADJUHand (five on the index finger and two on the casing). Their relative positions were used to approximate the location of each phalanx and calculate the corresponding joint angles (see Fig. 2). For abduction and circumduction only two points per finger were required. During motion capture testing, the ADJUHand was mounted on different fixtures to prevent translational movements while its fingers were actively moved (see Fig. 2).

To achieve flexion of the index finger without the risk of obscuring the optical markers, the tendons and routing structures of the stiffness system were repurposed. By removing the spring and screw assembly and extending the tendons in the proximal direction, they were routed out of the ADJUHand through the screw openings. By pulling on the palmar tendon, a flexion movement of the finger was induced (see Fig. 2).

#### F. Finger Stiffness Evaluation with Force Measurements

To evaluate the adjustability of the stiffness system, the resistive force was measured during finger flexion and extension in three configurations representing the minimum and

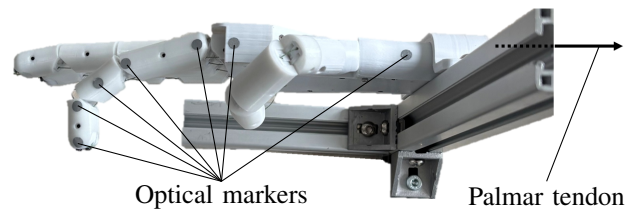


Fig. 2. Motion capturing setup for index finger flexion. The ADJUHand is fixed in a mounting frame with optical markers attached to the phalanges and hand casing. The arrow indicates the actuated palmar tendon.

maximum achievable stiffness. Measurements were carried out on the index finger as a representative example, since the other fingers were expected to show similar behavior. In the first configuration, both the palmar and dorsal tendons were set to minimal tension. In the second configuration, the dorsal tendon was maximally pretensioned while the palmar tendon remained at minimal tension. In the third configuration, the palmar tendon was maximally pretensioned while the dorsal tendon was kept at minimal tension.

For each configuration the force required to flex or extend the finger was measured using a simple exoskeleton setup. The exoskeleton consisted of a hand band and a finger component of the cable-driven exoskeleton *GraspAgain* [12], [22] (see Fig. 3). The force required to move the finger through pulling of the actuation cables was measured using a *Sauter FK100* force meter, which was set up to display the highest measured value detected during the measurement.

The same test exoskeleton also allowed for reference measurements on five healthy individuals (three male, aged 22–28 years; two female, aged 21–22 years) and two individuals with hand paralysis (both female; 43 years, complete cervical spinal cord injury at C5, AIS A; 57 years, spinal cord ischemia at C5 with partial preservation of function down to S1, AIS D).

Each configuration of the ADJUHand and each participant was measured five times. For analysis, the median and interquartile range (upper and lower quartiles) of these five measurements were calculated.

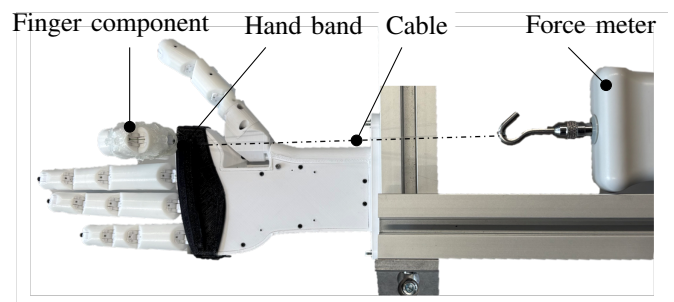


Fig. 3. Finger stiffness measurement setup. The ADJUHand is fixed on a mount, and a simple test exoskeleton (hand band and finger component) is used together with a force meter to actuate the exoskeleton cables along the palmar side for flexion resistance (or along the dorsal side for extension resistance, not shown) and to measure the maximal resistance force for different tendon configurations.

### G. Functionality Evaluation with an Exoskeleton

Since the primary purpose of the ADJUHand is to be used during testing phases of exoskeleton development, experiments were conducted to examine whether the ADJUHand can be controlled and moved through the forces generated by a hand exoskeleton. For this, the updated version of the hand exoskeleton *GraspAgain* [12], [22], was used to carry out movement and grasping tests. Before interacting with any objects, simple opening and closing movements of the ADJUHand were performed to verify basic actuation. Subsequently, different objects were grasped, lifted, held, and released using only the forces transmitted by the exoskeleton. The objects selected were a tennis ball (58 g), a Rubik's Cube (102 g), and a filled plastic water bottle (337 g).

### III. RESULTS

To assess the potential of a simple, safe and adjustable anthropomorphic hand model for realistic exoskeleton evaluation, we developed the ADJUHand. Fabricated almost entirely via 3D-printing, it incorporates adjustable finger stiffness and configurable finger abduction and adduction. We conducted kinematic analysis using motion capturing, performed comparative stiffness measurements against healthy and impaired hands, and validated the model's compatibility with a state of the art hand exoskeleton.

#### A. Finger Kinematics

To evaluate how closely the ADJUHand replicates human finger motion, finger joint angles were measured using motion capturing. The flexion angles of the index finger joints were  $85.23^\circ$  at the metacarpophalangeal (MCP) joint,  $84.29^\circ$  at the proximal interphalangeal (PIP) joint, and  $80.45^\circ$  at the distal interphalangeal (DIP) joint. Together, these contribute to a maximum total flexion angle of  $249.97^\circ$  for the index finger (see Tab. I). Compared to anatomical data from healthy adults, the ADJUHand's joint angles lie between the functional and passive ranges of motion, demonstrating realistic, human-like flexion within physiologically relevant limits. Moreover, the motion capture trajectories confirm that index finger flexion closely follows anatomical movement patterns (see Fig. 4a) [23].

The measured abduction angles of the long fingers were  $20.59^\circ$  for the index finger,  $0.00^\circ$  for the middle finger,  $12.97^\circ$  for the ring finger, and  $26.14^\circ$  for the little finger, generally falling short of the anatomical range of motion except for the index finger (see Tab. I, Fig. 4b) [24]. The thumb exhibited a circumduction range of  $93.44^\circ$ , which is consistent with the anatomical range of motion [25].

#### B. Finger Stiffness

To validate the finger stiffness system of the ADJUHand, maximum flexion and extension resistance forces were measured using a simple cable-driven exoskeleton, with a force meter attached directly to the actuation cable. The ADJUHand showed an adjustable finger resistance force range of 4.7 – 11.1 N for flexion and 3.6 – 7.31 N for

TABLE I  
FLEXION AND ABDUCTION ANGLES OF THE ADJUHAND COMPARED TO THE ANATOMICAL ANGLES OF HEALTHY ADULTS

Joint	Flexion Angle in $^\circ$			Finger	Abduct. Angle in $^\circ$	
	ADJU Hand	funct ROM [26]	pass ROM [26]		ADJU Hand	anat ROM [24]
MCP	85.23	73.00	100.00	Index	20.59	13.00
PIP	84.29	86.00	105.00	Middle	0.00	7.00
DIP	80.45	61.00	85.00	Ring	12.97	15.00
Total Arc	249.97	208.00	290.00	Little	26.14	29.00

Abbreviations: MCP = metacarpophalangeal joint, PIP = proximal interphalangeal joint, DIP = distal interphalangeal joint, ROM = range of motion, funct = functional, pass = passive, anat = anatomical.

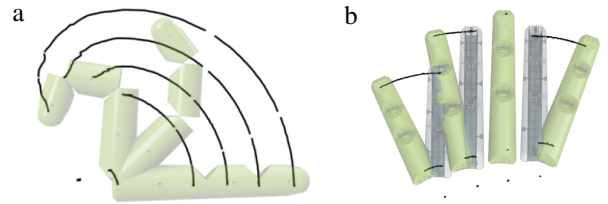


Fig. 4. ADJUHands finger movements from motion capturing. (a) Flexion trajectories of the index finger. (b) Abduction trajectories of the long finger.

extension across different tensioning configurations. Reference measurements on healthy and paralyzed human hands (all without known increased joint stiffness) most closely matched the ADJUHand with minimal dorsal and palmar pretension (see Fig. 5).

#### C. Functionality as Testing Device

To assess the operational performance of the ADJUHand, the state of the art hand exoskeleton *GraspAgain* [12], [22] was used to perform simple flexion and extension movements, which the ADJUHand reliably followed. After verifying these movements, grasping tasks with various objects including a bottle, a Rubik's Cube, and a tennis ball demonstrated that the ADJUHand accurately transmitted the exoskeleton's forces to achieve successful grasp, lift, and release of each object (see Fig. 6).

### IV. DISCUSSION

Our findings demonstrate that the ADJUHand, produced primarily through 3D-printing, successfully replicates essential biomechanical characteristics of the human hand. Its adjustable stiffness and abduction capabilities facilitate realistic and safe testing environments for hand exoskeletons.

Comparison of the flexion angles measured for the ADJUHand with anatomical data shows that the design exceeds the functional range of motion but does not fully reach the passive range observed in healthy hands (see Tab. I) [26]. Results from other passive hand models show variation, with [9] reporting higher flexion angles for the MCP and PIP joints ( $120^\circ$ ) but no data for the DIP joint and total arc, [10] providing only joint trajectories without specific

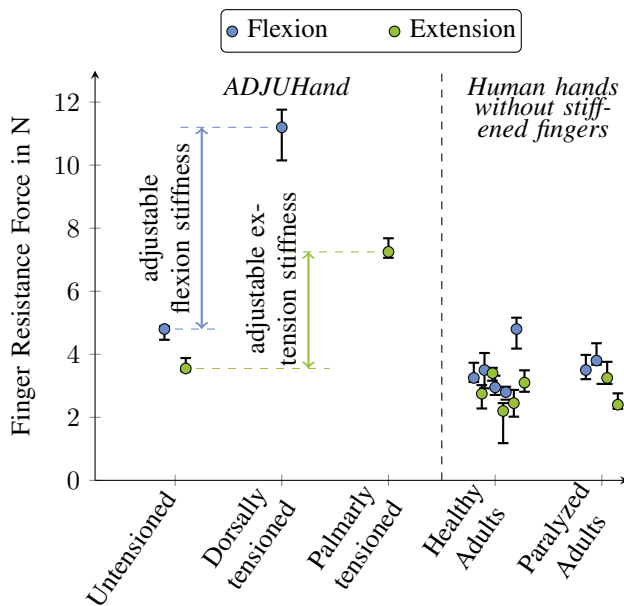


Fig. 5. Finger stiffness measurements for the ADJUHand and human fingers under different palmar and dorsal pretension configurations using a test exoskeleton. The untensioned ADJUHand fingers exhibit stiffness closest to that of human fingers. Dorsal or palmar pretension of the internal tendons of the ADJUHand allows tuning of flexion and extension stiffness. Each point represents the median maximum resistance force from five trials required to flex (blue) or extend (green) a finger with an exoskeleton. Vertical bars indicate the interquartile range (25th–75th percentile). Measurements were performed on the ADJUHands finger (left) and compared with data from five healthy and two paralyzed adults without increased finger stiffness (right).

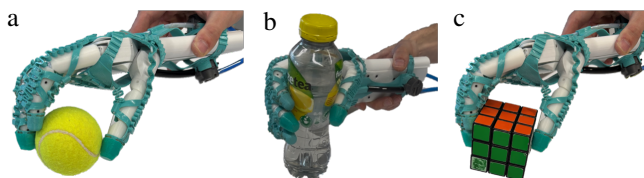


Fig. 6. Grasping tests of the ADJUHand with *GraspAgain* [12], [22]. (a) tennis ball. (b) bottle. (c) Rubik's Cube.

angle values, and [16] not reporting any reached angles. Since hand exoskeletons are primarily intended to restore functional motion, the performance of the ADJUHand can be considered sufficient for its intended purpose.

In contrast, the ADJUHand does not reach the full anatomical range of motion for finger abduction with the exception of the index finger (see Table I) [24] due to spatial constraints within the casing. The passive models from [9], [10], [16] claim configurable abduction but report no specific values. Since abduction is not essential for basic grasping and is rarely actively controlled in exoskeletons, the available range of motion of the ADJUHand is sufficient and simplifies both donning and doffing of the exoskeleton devices.

The ADJUHand's thumb circumduction closely matches anatomical values reported by [25], achieving  $93.44^\circ$ , slightly exceeding the  $90^\circ$  anatomical pronation. This full range of thumb motion is crucial for testing different types of grasps. In contrast, [9] report no thumb motion, while [16] and [10]

claim thumb circumduction but do not provide any numbers.

Comparison with anatomical finger movement trajectories [23] shows that the flexion trajectory of the ADJUHand closely mirrors natural finger motion (see Fig. 4). However, increasing the tension on the dorsal tendons caused a non-anatomical pattern, where MCP joint flexion occurred before that of the PIP and DIP joints. This deviation likely results from an imbalance in tendon forces and could potentially be corrected by increasing the palmar tendon tension. Furthermore, in this configuration, the finger could not reach full flexion without risking damage to the test exoskeleton, likely due to its limited range of motion.

The force measurements confirm the functionality of the ADJUHand's adjustable finger stiffness mechanism. Compared to data from five healthy and two paralyzed subjects without known increases in finger stiffness, the minimum stiffness achievable with the ADJUHand falls within a similar range (see Fig. 5). Although resistance forces in paralyzed subjects with stiffened fingers were not measured, they are expected to be higher and can be simulated by increasing the ADJUHand's stiffness. Our measurements show that both flexion and extension resistance can be doubled. To the best of the authors' knowledge, no other system currently allows adjusting finger stiffness.

Using the hand exoskeleton *GraspAgain*, the ADJUHand proved to be a feasible test platform, achieving successful grasping of various objects (see Fig. 6) consistent with the models from [9] and [16]. However, the open joint design revealed limitations. The fixation strap of the hand exoskeleton occasionally slipped into the the MCP joint on the palmar side, blocking full flexion of the little finger, and the exoskeleton finger component sometimes caught on the dorsal side of the PIP joint during extension. These issues arise from the edge and open joint design of the ADJUHand and from the *GraspAgain* exoskeleton, which is an open, lightweight structure rather than a closed glove.

## V. CONCLUSION

This paper introduces the ADJUHand, a passive, additively manufactured hand model designed to evaluate hand exoskeletons under safe and physiologically realistic conditions. It reproduces key biomechanical features of the human hand, including anatomically plausible movement ranges, tunable finger stiffness, and adjustable finger abduction. Motion capturing analysis confirmed a flexion range of motion exceeding functional requirements for daily grasping.

The integrated adjustable stiffness mechanism allows replication of various finger conditions, such as increased resistance in spasticity or contractures. Evaluation with a state of the art hand exoskeleton demonstrated suitability for functional assessments. Limitations include mechanical interference between casing and exoskeleton and the inability to modulate stiffness at individual joints. Consequently, stiffness in Nm/rad was not measured for individual joints, and only overall finger stiffness was assessed.

Future work will focus on closing the open joint design with flexible TPU elements (skin layer) to minimize the

potential for interference with exoskeleton devices. Planned studies with patients exhibiting contractures or spasticity will assess the physiological validity of the stiffness mechanism. Sensor integration for joint angle and force measurement is further envisioned to enable objective biomechanical evaluation of hand exoskeletons.

## REFERENCES

- [1] V. L. Feigin, M. Brainin, B. Norrving, S. Martins, R. L. Sacco, W. Hacke, M. Fisher, J. Pandian, and P. Lindsay, "World Stroke Organization (WSO): Global Stroke Fact Sheet 2022," *International Journal of Stroke*, vol. 17, no. 1, pp. 18–29, Jan. 2022. [Online]. Available: <https://journals.sagepub.com/doi/10.1177/17474930211065917>
- [2] W. Ding, S. Hu, P. Wang, H. Kang, R. Peng, Y. Dong, and F. Li, "Spinal Cord Injury: The Global Incidence, Prevalence, and Disability From the Global Burden of Disease Study 2019," *Spine*, vol. 47, no. 21, pp. 1532–1540, Nov. 2022. [Online]. Available: <https://www.ncbi.nlm.nih.gov/pmc/articles/PMC9554757/>
- [3] G. J. Snook, M. J. IJzerman, H. J. Hermens, D. Maxwell, and F. Biering-Sorensen, "Survey of the needs of patients with spinal cord injury: impact and priority for improvement in hand function in tetraplegics," *Spinal Cord*, vol. 42, no. 9, pp. 526–532, Sep. 2004. [Online]. Available: <https://www.nature.com/articles/3101638>
- [4] Q. Tang, X. Yang, M. Sun, M. He, R. Sa, K. Zhang, B. Zhu, and T. Li, "Research trends and hotspots of post-stroke upper limb dysfunction: a bibliometric and visualization analysis," *Frontiers in Neurology*, vol. 15, p. 1449729, Oct. 2024. [Online]. Available: <https://www.ncbi.nlm.nih.gov/pmc/articles/PMC11479973/>
- [5] B. Noronha and D. Accoto, "Exoskeletal Devices for Hand Assistance and Rehabilitation: A Comprehensive Analysis of State-of-the-Art Technologies," *IEEE Transactions on Medical Robotics and Bionics*, vol. 3, no. 2, pp. 525–538, May 2021. [Online]. Available: <https://ieeexplore.ieee.org/document/9372328/>
- [6] F. Aggogeri, T. Mikolajczyk, and J. O'Kane, "Robotics for rehabilitation of hand movement in stroke survivors," *Advances in Mechanical Engineering*, vol. 11, no. 4, p. 1687814019841921, Apr. 2019, publisher: SAGE Publications. [Online]. Available: <https://doi.org/10.1177/1687814019841921>
- [7] C. Walsh, "Human-in-the-loop development of soft wearable robots," *Nature Reviews Materials*, vol. 3, no. 6, pp. 78–80, May 2018. [Online]. Available: <https://www.nature.com/articles/s41578-018-0011-1>
- [8] S. Grosu, L. De Rijke, V. Grosu, J. Geeroms, B. Vanderboght, D. Lefeber, and C. Rodriguez-Guerrero, "Driving Robotic Exoskeletons Using Cable-Based Transmissions: A Qualitative Analysis and Overview," *Applied Mechanics Reviews*, vol. 70, no. 6, p. 060801, Nov. 2018. [Online]. Available: <https://asmedigitalcollection.asme.org/appliedmechanicsreviews/article/doi/10.1115/1.4042399/367041/Driving-Robotic-Exoskeletons-Using-CableBased>
- [9] S. N. Yousaf, V. S. Joshi, J. E. Britt, C. G. Rose, and M. K. O'Malley, "Design and Characterization of a Passive Instrumented Hand," *ASME Letters in Dynamic Systems and Control*, vol. 1, no. 1, p. 011007, Jan. 2021. [Online]. Available: <https://asmedigitalcollection.asme.org/lettersdynsys/article/doi/10.1115/1.4046449/1074852/Design-and-Characterization-of-a-Passive>
- [10] C. Brogi, A. Raggi, N. Secciani, Y. Volpe, and A. Ridolfi, "A Passive, Customizable and Kinetically-Accurate Hand Replica for Testing Assistive and Rehabilitative Hand Exoskeleton Systems," in *Advances in Italian Mechanism Science*, V. Niola, A. Gasparetto, G. Quaglia, and G. Carbone, Eds. Cham: Springer International Publishing, 2022, pp. 505–513.
- [11] R. Ribeiro, C. Leão, S. Costa, and V. Silva, "Ergonomic Evaluation Methods for Hand Exoskeleton Prototypes: A Scoping Study," 2025. [Online]. Available: <https://openaccess.cms-conferences.org/publications/book/978-1-964867-36-6/article/978-1-964867-36-6.67>
- [12] J. Walter, P. Rosmanith, D. S. De Oliveira, S. Reitelshofer, A. Del Vecchio, and J. Franke, "Proportional Control of a Soft Cable-Driven Exoskeleton via a Myoelectrical Interface Enables Force-Controlled Finger Motions," in *2022 9th IEEE RAS/EMBS International Conference for Biomedical Robotics and Biomechatronics (BioRob)*. Seoul, Korea, Republic of: IEEE, Aug. 2022, pp. 1–6. [Online]. Available: <https://ieeexplore.ieee.org/document/9925334/>
- [13] J. Diong, L. A. Harvey, L. K. Kwah, J. Eyles, M. J. Ling, M. Ben, and R. D. Herbert, "Incidence and predictors of contracture after spinal cord injury—a prospective cohort study," *Spinal Cord*, vol. 50, no. 8, pp. 579–584, Aug. 2012, publisher: Nature Publishing Group. [Online]. Available: <https://www.nature.com/articles/sc201225>
- [14] X. Q. Shi, H. L. Heung, Z. Q. Tang, K. Y. Tong, and Z. Li, "Verification of Finger Joint Stiffness Estimation Method With Soft Robotic Actuator," *Frontiers in Bioengineering and Biotechnology*, vol. 8, Dec. 2020, publisher: Frontiers. [Online]. Available: <https://www.frontiersin.org/journals/bioengineering-and-biotechnology/articles/10.3389/fbioe.2020.592637/full>
- [15] K. Gilday, J. Hughes, and F. Iida, "Wrist-driven passive grasping: interaction-based trajectory adaptation with a compliant anthropomorphic hand," *Bioinspiration & Biomimetics*, vol. 16, no. 2, p. 026024, Mar. 2021, publisher: IOP Publishing. [Online]. Available: <https://dx.doi.org/10.1088/1748-3190/abe345>
- [16] J. Park, I. Hwang, and W. Lee, "Wearable Robotic Glove Design Using Surface-Mounted Actuators," *Frontiers in Bioengineering and Biotechnology*, vol. 8, Sep. 2020, publisher: Frontiers. [Online]. Available: <https://www.frontiersin.org/journals/bioengineering-and-biotechnology/articles/10.3389/fbioe.2020.548947/full>
- [17] M. Vergara, M. J. Agost, and V. Gracia-Ibáñez, "Dorsal and palmar aspect dimensions of hand anthropometry for designing hand tools and protections," *Human Factors and Ergonomics in Manufacturing & Service Industries*, vol. 28, no. 1, pp. 17–28, 2018, eprint: <https://onlinelibrary.wiley.com/doi/pdf/10.1002/hfm.20714>. [Online]. Available: <https://onlinelibrary.wiley.com/doi/abs/10.1002/hfm.20714>
- [18] S. D. Childress, K. M. Coffey, E. Benson, G. Gupta, S. Rajulu, and K. S. Young, "OCHMO-HB-004 ANTHROPOMETRY, BIOMECHANICS, AND STRENGTH."
- [19] B. Buchholz, T. J. Armstrong, and S. A. Goldstein, "Anthropometric data for describing the kinematics of the human hand," *Ergonomics*, vol. 35, no. 3, pp. 261–273, Mar. 1992. [Online]. Available: <http://www.tandfonline.com/doi/abs/10.1080/00140139208967812>
- [20] A. Unsworth, "Tribology of Human and Artificial Joints," *Proceedings of the Institution of Mechanical Engineers, Part H: Journal of Engineering in Medicine*, vol. 205, no. 3, pp. 163–172, Sep. 1991. [Online]. Available: [https://journals.sagepub.com/doi/10.1243/PIME\\_PROC.1991.205.287.02](https://journals.sagepub.com/doi/10.1243/PIME_PROC.1991.205.287.02)
- [21] S.-H. Kim, H. In, J.-R. Song, and K.-J. Cho, "Force characteristics of rolling contact joint for compact structure," in *2016 6th IEEE International Conference on Biomedical Robotics and Biomechatronics (BioRob)*, Jun. 2016, pp. 1207–1212, iSSN: 2155-1782. [Online]. Available: <https://ieeexplore.ieee.org/document/7523795>
- [22] N. Weber, J. Walter, D. Braun, A. Del Vecchio, and J. Franke, "Compact and Lightweight Cable Decoupling Unit for Bio-Inspired Tendon Drives in Wearable Robots," in *2024 10th IEEE RAS/EMBS International Conference for Biomedical Robotics and Biomechatronics (BioRob)*. Heidelberg, Germany: IEEE, Sep. 2024, pp. 1140–1145. [Online]. Available: <https://ieeexplore.ieee.org/document/10719892/>
- [23] A. A. Mohd Faudzi, J. Ooga, T. Goto, M. Takeichi, and K. Suzumori, "Index Finger of a Human-Like Robotic Hand Using Thin Soft Muscles," *IEEE Robotics and Automation Letters*, vol. 3, no. 1, pp. 92–99, Jan. 2018. [Online]. Available: <https://ieeexplore.ieee.org/document/7993072>
- [24] J. Coupier, S. Hamoudi, S. Telese-Izzi, V. Feipel, M. Rooze, and S. Van Sint Jan, "A novel method for in-vivo evaluation of finger kinematics including definition of healthy motion patterns," *Clinical Biomechanics*, vol. 31, pp. 47–58, Jan. 2016. [Online]. Available: <https://linkinghub.elsevier.com/retrieve/pii/S0268003315002636>
- [25] M. Tonkin, "Thumb opposition: its definition and my approach to its measurement," *Journal of Hand Surgery (European Volume)*, vol. 45, no. 3, pp. 315–317, Mar. 2020, publisher: SAGE Publications Ltd STM. [Online]. Available: <https://doi.org/10.1177/1753193419889504>
- [26] M. C. Hume, H. Gellman, H. McKellop, and R. H. Brumfield, "Functional range of motion of the joints of the hand," *The Journal of Hand Surgery*, vol. 15, no. 2, pp. 240–243, Mar. 1990. [Online]. Available: <https://linkinghub.elsevier.com/retrieve/pii/S036350239090102W>